



TITLE:

Origins of multisynaptic projections from the basal ganglia to the forelimb region of the ventral premotor cortex in macaque monkeys

AUTHOR(S):

Ishida, Hiroaki; Inoue, Ken-ichi; Takada, Masahiko; Hoshi, Eiji

CITATION:

Ishida, Hiroaki ...[et al]. Origins of multisynaptic projections from the basal ganglia to the forelimb region of the ventral premotor cortex in macaque monkeys. *European Journal of Neuroscience* 2016, 43(2): 258-269

ISSUE DATE:

2016-01

URL:

<http://hdl.handle.net/2433/218581>

RIGHT:

This is the peer reviewed version of the following article: [Ishida, H., Inoue, K.-i., Takada, M., Hoshi, E. (2016), Origins of multisynaptic projections from the basal ganglia to the forelimb region of the ventral premotor cortex in macaque monkeys. *European Journal of Neuroscience*, 43: 258–269], which has been published in final form at <https://doi.org/10.1111/ejn.13127>. This article may be used for non-commercial purposes in accordance with Wiley Terms and Conditions for Self-Archiving; この論文は出版社版ではありません。引用の際には出版社版をご確認ください。 ; This is not the published version. Please cite only the published version.

Research Reports/Neurosystem

**Origins of multisynaptic projections from the basal ganglia to the forelimb region
of the ventral premotor cortex in macaque monkeys**

BG projections to the forelimb region of PMv

Hiroaki Ishida^{1*}, Ken-ichi Inoue^{2*}, Masahiko Takada², Eiji Hoshi¹

¹Frontal Lobe Function Project, Tokyo Metropolitan Institute of Medical Science,
Setagaya-ku, Tokyo, Japan

²Systems Neuroscience Section, Primate Research Institute, Kyoto University, Inuyama,
Aichi, Japan

*These authors contributed equally to this work.

Co-corresponding Authors:

Dr. Masahiko Takada

Systems Neuroscience Section, Primate Research Institute, Kyoto University, 41-2
Kanrin, Inuyama, Aichi 484-8506, Japan
e-mail: takada.masahiko.7x@kyoto-u.ac.jp

Dr. Eiji Hoshi

Frontal Lobe Function Project, Tokyo Metropolitan Institute of Medical Science, 2-1-6
Kamikitazawa, Setagaya-ku, Tokyo 156-8506, Japan
e-mail: hoshi-ej@igakuken.or.jp

Manuscript contains 10 figures, 1 table and 40 pages.

Number of words: Manuscript, 9615; Abstract, 250; Introduction, 523.

Keywords: rabies virus, globus pallidus, striatum, subthalamic nucleus, substantia nigra

For Peer Review

Abstract

The ventral premotor cortex (PMv), occupying the ventral aspect of area 6 in the frontal lobe, has been implicated in action planning and execution based on visual signals. Although the PMv has been characterized by cortico-cortical connections with specific subregions of the parietal and prefrontal cortical areas, a topographical input/output organization between the PMv and the basal ganglia (BG) still remains elusive. In the present study, we employed retrograde transneuronal labeling with rabies virus to identify the origins of multisynaptic projections from the BG to the PMv. We injected the virus into the forelimb region of the PMv, identified in the ventral aspect of the genu of the arcuate sulcus, in macaque monkeys. The survival time after the virus injection was set to allow either the second- or third-order neuron labeling across two or three synapses. The second-order neurons were observed in the ventral portion (primary motor territory) and the caudodorsal portion (higher-order motor territory) of the internal segment of the globus pallidus. Subsequently, the third-order neurons were distributed in the putamen caudal to the anterior commissure, including both the primary and the higher-order motor territories, and in the ventral striatum (limbic territory). In addition, they were found in the dorsolateral portion (motor territory) and

ventromedial portion (limbic territory) of the subthalamic nucleus and in the external segment of the globus pallidus including both the limbic and motor territories. These findings indicate that the PMv receives diverse signals from the primary motor, higher-order motor, and limbic territories of the BG.

For Peer Review

Introduction

The premotor (PM) cortex in primates, the rostral part of the frontal motor cortex corresponding to Brodmann area 6, plays a central role in the visual guidance of motor behavior (Halsband & Passingham, 1985; Wise, 1985; García-Cabezas & Barbas, 2014; Yamawaki et al., 2014; Barbas & García-Cabezas, 2015). Seminal anatomical works of the monkey brain have revealed that the PM is subdivided into two large sectors based on the cytoarchitecture (Matelli *et al.*, 1985, 1986; Barbas & Pandya, 1987): one is a dorsal region (PMd), lying dorsal to the spur of the arcuate sulcus, and another is a ventral region (PMv), lying ventral to the spur. Electrical stimulation and mapping studies showed that there is a forelimb region in each of the PMd and PMv (Gentilucci *et al.*, 1988; Godschalk *et al.*, 1995; Raos *et al.*, 2003; Aflalo and Graziano, 1996; Maranesi *et al.*, 2012). Single cell recoding studies have revealed that the PMd and PMv are involved in reaching and grasping movements in an area-specific manner (Kurata & Wise, 1988; Caminiti *et al.*, 1991; Boussaoud & Wise, 1993a, b; Kurata, 1993; Scott *et al.*, 1997; Kurata & Hoshi, 2002; Raos *et al.*, 2004, 2006; Umiltà *et al.*, 2007; Yamagata *et al.*, 2009). By summarizing a large body of evidence, Hoshi and Tanji (2007) have

proposed that the PMd plays a major role in action planning based on sensory-motor associations (indirect [conceptual] specification of action), whereas the PMv plays a major role in reaching and grasping a target object (direct guidance of limb movements). Actually, the specific functional deficits that result from PMd/PMv lesions endorse these notions (Rizzolatti *et al.*, 1983; Kurata & Hoffman, 1994; Kurata & Hoshi, 1999; Schieber, 2000; Fogassi *et al.*, 2001).

The functional specializations between the PMd and the PMv may originate from distinct anatomical connectivity. Actually, these areas are interconnected with distinct subregions of the parietal and prefrontal cortical areas (Wise *et al.*, 1997; Matelli *et al.*, 1998; Rizzolatti *et al.*, 1998; Luppino *et al.*, 1999; Petrides & Pandya, 1999). In addition to the connectivity within the cerebral cortex, it is most likely that neural networks linking these forelimb regions with the basal ganglia (BG) play functionally crucial roles, given that neurons in the BG code a variety of signals for planning and execution of reaching movement (Iansek & Porter, 1980; DeLong *et al.*, 1985) and their dysfunctions cause severe deficits in movement (Alexander & Crutcher, 1990; Parent & Hazrati, 1995a, b).

In the present study we made an attempt to investigate the distributions of BG neurons giving rise to output projections to the forelimb region of the PMv, as an extension of our previous anatomical study that has revealed the origins of multisynaptic projections from the BG to the corresponding region of the PMd (Saga *et al.*, 2011). We employed retrograde transneuronal labeling with rabies virus (CVS-11) to identify the cellular origins of multisynaptic projections from the BG structures to the forelimb region of the PMv in macaque monkeys. We here show that the forelimb region of the PMv receives multisynaptic inputs from the primary motor territory, higher-order motor territory, and limbic territory of the BG.

Materials and methods

We used four male macaque monkeys (*Macaca fuscata*, weighing 5.4-6.9 kg; provided by the Primate Research Institute, Kyoto University, Table 1). The experimental protocol was approved by the Animal Welfare and Animal Care Committee of the Primate Research Institute, Kyoto University, and all experiments were conducted in accordance with the Guideline for the Care and Use of Animals of

the Primate Research Institute, Kyoto University.

Surgical procedures

Monkeys were subjected to general anesthesia induced with ketamine hydrochloride (10 mg/kg, i.m.) and maintained with sodium pentobarbital (20 mg/kg, i.v.). During the surgical operation, monkeys were kept hydrated with lactated Ringer's solution (i.v.). An antibiotic (Rocephin; 75 mg/kg, i.m.) and an analgesic (Buprenex; 0.01 mg/kg, i.m.) were administered at the time of initial anesthesia. Each monkey's head was secured in a stereotaxic frame, and the skin and muscle were retracted to expose the skull over the right hemisphere. A craniotomy was made over the right frontal cortex, and the dura mater was cut to expose the superior and inferior limbs and the genu of the arcuate sulcus, which allowed us to visually inspect the tracer injection sites at the cortical surface. After confirming this, we proceeded with tracer injections.

Viral injections

The rabies virus (CVS-11 strain; 1.0×10^8 focus-forming units/ml) was derived from

the Centers for Disease Control and Prevention (Atlanta, GA, USA) and donated by Dr. S. Inoue (The National Institute of Infectious Diseases, Tokyo, Japan). For viral injections, we used the same method as described in our previous reports (Hashimoto *et al.*, 2010; Saga *et al.*, 2011; Takahara *et al.*, 2012). Two tracks of injections of rabies virus were made into the PMv of each of the four monkeys (Fig. 1, Table 1). The injection sites were determined based on the results of our prior studies showing that the subdivision of the PMv located just ventral to the genu of arcuate sulcus plays a crucial role in reaching movement (Hoshi & Tanji, 2002, 2006, 2007; Yamagata *et al.*, 2009, Fig.1B, C). A viral suspension was slowly injected through a 10- μ l Hamilton microsyringe. Along each injection track, viral deposits were placed at two different depths: 3 and 2 mm below the cortical surface. At each depth, 0.5 μ l of the viral suspension was deposited. When injections were complete, the dura mater and bone flap were repositioned, and the scalp incision was closed.

Histology

After survival periods of 3-4 days after viral injection, monkeys were deeply

anesthetized with an overdose of sodium pentobarbital (50 mg/kg, i.v.) and transcardially perfused with 10% formalin in 0.1 M phosphate buffer (pH 7.4). The fixed brains were removed from the skull, postfixed in the same fresh fixative overnight at 4°C, and placed into 0.1 M phosphate buffer (pH 7.4) containing 30% sucrose. Coronal sections were then cut serially at 50 µm thickness on a freezing microtome. Every sixth section was processed for immunohistochemical staining for rabies virus by means of the standard avidin-biotin-peroxidase complex method. Following immersion in 1% skimmed milk, the sections were incubated overnight with rabbit anti-rabies virus antibody (donated by Dr. S. Inoue) in 0.1 M phosphate-buffered saline (pH 7.4) containing 0.1% Triton X-100 and 1% normal goat serum. The sections were then placed in the same fresh incubation medium containing biotinylated goat anti-rabbit IgG antibody (diluted at 1:200; Vector Laboratories, Burlingame, CA, USA), followed by the avidin-biotin-peroxidase complex kit (ABC Elite; Vector Laboratories). To visualize the antigen, the sections were reacted in 0.05 M Tris-HCl buffer (pH 7.6) containing 0.04% diaminobenzidine, 0.04% nickel chloride, and 0.002% hydrogen peroxide. The sections were mounted onto gelatin-coated glass slides and then examined under the

light microscope (Nikon Eclipse 80i, Tokyo, Japan).

Analytical procedures

We digitized the outline of the nuclei of the BG and the location of labeled neurons with the MD-Plot 5 system (Accustage, Shoreview, MN, USA) attached to the microscope system. Neuronal labeling was plotted on tracings of equidistant coronal sections (separated by 300- μ m) throughout the BG. To examine the distribution and density of labeled neurons in the internal and external segments of the globus pallidus (GPi and GPe), we created two-dimensional density maps with a custom-made program that operates on Matlab (Mathworks, Natick, MA, USA). To create the density maps of the GPi, we first drew a curved line on each coronal section along the border between the inner and the outer portion of the GPi (Fig. 5A). Subsequently, labeled GPi neurons were projected onto the line, and both the line and the labeled neurons were unfolded and aligned on the ventral edges of the nucleus (Fig. 5B). Finally, to construct the density maps, we aligned the labeled neurons in each section (with 300- μ m intervals) in the rostrocaudal direction and counted the number of the labeled neurons in each of 300

$\times 300 \mu\text{m}^2$ bins. To create the density maps of the GPe, we drew a curved line on each coronal section midway between the medial and the lateral outline of the GPe (Fig. 8A). The subsequent unfolding procedures (Fig. 8B) were as for the GPi. A color code in each map of the GPi and GPe was assigned to each bin to indicate the number of labeled neurons included (Figs. 5C, D and 8C, D).

Safety issues

Experiments involving the rabies virus were performed in a special primate laboratory (biosafety level 2) designated for in vivo infectious experiments. Throughout the experiments, the monkeys were housed in individual cages that were installed inside a special biosafety cabinet. To avoid accidental infection with the virus, all investigators received immunizations beforehand and wore protective clothing during the experimental sessions. Equipment was disinfected with 80% (v/v) ethanol after each experimental session, and waste was autoclaved prior to disposal.

Results

Rabies injections into the PMv

The injection sites of rabies virus were determined according to the results from our previous electrophysiological studies (see Hoshi & Tanji, 2002, 2006; Yamagata *et al.*, 2009). In these studies, we found that PMv neurons located in the ventral aspect of the genu of the arcuate sulcus preferentially represent the target site, regardless of the right or left arm use, during the preparation of reaching movement. Based on this finding, two injection tracks (approximately 1 mm apart) were targeted at this portion of the PMv; the sites were situated 1–2 mm posterior to the genu of the arcuate sulcus and 1–2 mm lateral to the spur of the arcuate sulcus (Fig. 1B-D). At the 3-day post-injection period, labeled neurons were densely distributed around the injection sites (Fig. 1E, F).

The survival time after the rabies injections was set to allow either the second-order or the third-order neuron labeling across two or three synapses, respectively: (1) the first-order neurons from the PMv were located in the ventral nuclei (e.g., VLo, VApc) and mediodorsal nucleus of the thalamus (Morel *et al.*, 2005); (2) the second-order and third-order neurons from the PMv were located in the BG 3 or 4 days after the rabies injections, respectively. For instance, Figure 2A, B show examples of labeled neurons

observed in the GPi and SNr at the 3-day post-injection period (second-order neurons).

Figure 2C shows examples of labeled neurons observed in the GPe at the 4-day

post-injection period (third-order neurons). Summary of the number of labeled neurons

for each nucleus is shown in Figure 3.

Origins of multisynaptic projections to the PMv from the GPi and SNr

Three days after the rabies injections into the PMv, the second-order neurons were seen in both the GPi and the SNr in two cases (Figs. 4 and 6). The number of labeled neurons in the outer portion of the GPi was 267 on average (257 cells in Case 1 and 277 cells in Case 2), while that in the inner portion of the GPi was 146 on average (111 cells in Case 1 and 181 cells in Case 2, Fig. 3). In order to examine the distribution of the labeled neurons within the GPi, two-dimensional density maps were made (Fig. 5A, B). These maps indicated that the origin of the projection to the PMv consisted of two parts of the GPi; one was the caudodorsal part, and the other was the ventral part (Fig. 5C, D).

Labeled neurons in the SNr were found widely throughout the entire rostrocaudal

extent of the nucleus (Fig. 6). At the rostral level, the labeled neurons were located in the dorsolateral part (Fig. 6A, B, A', B'), while in the caudal two-thirds of the SNr, the labeled neurons were distributed primarily in the central part (Fig. 6C-F, C'-F'). The number of labeled neuron in the SNr was 203 on average (307 cells in Case 1 and 99 cells in Case 2, Fig. 3).

Origins of multisynaptic projections to the PMv from the GPe, STN, and striatum

By extending the post-injection survival period to 4 days, we detected neuronal labeling in the GPe, STN, and striatum. In the GPe, labeled neurons were widely distributed over the nucleus (Fig. 7). In order to examine the distribution of labeled neurons, two-dimensional density maps of the GPe were made in two cases. In both cases, the labeled neurons were located not only in the rostroventral portion, but also in the dorsoventrally middle portion at the caudal level (Fig. 8). The number of labeled neurons in the GPe was 2,562 on average (2,332 cells in Case 3 and 2,792 cells in Case 4, Fig. 3).

Labeled neurons in the STN were observed extensively throughout the entire

rostrocaudal extent of the nucleus (Fig. 9). The labeled neurons were distributed primarily in the central to dorsolateral portions of the caudal half of the nucleus (Fig. 9C-F, C'-F'). Another focus of the labeled neurons was seen in the ventromedial portion mainly at the rostral level of the nucleus (Fig. 9A, B, A', B'). The number of labeled neurons in the STN was 1,679 on average (1,583 cells in Case 3 and 1,774 cells in Case 4, Fig. 3).

In the striatum, a large number of labeled neurons were observed (Fig. 10). At the level rostral to the anterior commissure (ac; Fig. 10A-C, A'-C'), labeled neurons were located in the ventral striatum. At the level caudal to the ac (Fig. 10D-F, D'-F'), labeled neurons were found at the dorsoventrally middle portion of the medial and lateral aspects of the putamen. Further, throughout the entire rostrocaudal extent of the striatum except for the anterior-most level (Fig. 10A-E, A'-E'), labeled neurons were continuously seen in the striatal cell bridge region and in adjacent regions of the caudate nucleus and the putamen. The number of labeled neuron in the caudate nucleus including the bridge region was 2,890 on average (3,431 cells in Case 3 and 2,289 cells in Case 4), and that in the putamen was 24,036 on average (27,815 cells in Case 3 and

20,256 cells in Case 4, Fig. 3).

Discussion

We examined the organization of multisynaptic projections from the BG to the forelimb region of the PMv in macaque monkeys. After injecting rabies virus into the PMv, we found the second-order neuron labeling in the GPi and SNr. Subsequently, the third-order neuron labeling occurred in the GPe, STN, and striatum. Our histological analysis of the distributions of rabies-labeled neurons revealed that the PMv primarily receives major input signals from multiple territories within each structure of the BG that have comprised the two distinct motor territories (i.e., the primary and higher-order motor territories) and the limbic territory.

Multisynaptic inputs to the PMv from the primary motor territory of the GPi and striatum

In the present study, we obtained many pieces of evidence indicating that the PMv receives inputs from the two distinct motor territories (i.e., the primary and higher-order

motor territories) of the BG. We first discuss the organization of the inputs from the primary motor territory.

We observed that two different parts of the GPi give rise to disynaptic projections to the PMv. The first part was located in the ventral aspect of the GPi. Several lines of evidence have shown that this ventral part is interconnected predominantly with the primary motor cortex (M1). First, anatomical studies using retrograde transsynaptic transport of neurotropic viruses have revealed that the ventral part of the GPi projects multisynaptically to the M1 via the motor thalamus (Hoover & Strick, 1993, 1999). Second, by examining the responses of GPi and GPe neurons to cortical and striatal electrical stimulations, Yoshida *et al.* (1993) identified pallidal neurons that receive inputs from the M1, PMv, PMd, the supplementary motor area (SMA), and the prefrontal cortex. They found that neurons in the ventral part of the GPi receive input preferentially from the M1. Third, Haber *et al.* (1990, 1993, 1995, 2000) have revealed that the ventrolateral GPi receives input from the dorsolateral putamen, which corresponds to the zone that receives major input from the arm region of the M1 (Takada *et al.*, 1998a, b; Kaneda *et al.*, 2002). These findings indicate that the PMv

receives disynaptic input from the primary motor territory located in the ventral aspect of the GPi. Within the striatum, the third-order neurons were distributed in the putamen caudal to the ac. One group of dense patches of labeled neurons was seen in the dorsoventrally middle portion of the lateral aspect of the putamen. It has been shown that this portion of the putamen receives major input from the arm region of the M1 (Zemanick *et al.*, 1991; Inase *et al.*, 1996b; Takada *et al.*, 1998a, b; Kaneda *et al.*, 2002). These observations indicate that the PMv receives input from the primary motor territory of the striatum. The overall results provide evidence that the PMv receives multisynaptic inputs from the primary motor territories of the GPi and striatum.

Multisynaptic inputs to the PMv from the higher-order motor territory of the GPi and striatum

The second part of the GPi that sends disynaptic projections to the PMv was identified in the caudodorsal aspect of the nucleus. The previous study of Yoshida *et al.* (1993) have revealed that neurons in the caudodorsal part of the GPi respond primarily to electrical stimulation of the PMd, SMA, the cingulate motor area, or PMv. In our

prior study, Saga *et al.* (2011) found that GPi neurons projecting to the PMdc (i.e., the caudal aspect of area F2) were located dorsal to those projecting to the M1 (Hoover & Strick, 1993,1999). Moreover, the neurons in the caudodorsal part of the GPi have been shown to project to the SMA across synapses (Akkal *et al.*, 2007). These findings suggest that this part of the GPi may correspond to a higher-order motor territory, and that the PMv receives input from such a territory across synapses. Within the striatum, a subset of the third-order neurons was distributed in the medial aspect of the putamen, including the striatal cell bridge region. Takada *et al.* (1998a, b) have revealed that this part of the striatum receives major inputs from the arm regions of the PMv, PMd, and SMA. In our prior study (Saga *et al.*, 2011), rabies injections into the PMdc produced retrograde neuronal labeling in the same striatal zone. These findings indicate that the medial aspect of the putamen corresponds to a higher-order motor territory, and that the PMv receives input from this striatal territory across synapses. The overall results provide evidence that the PMv receives inputs from the higher-order motor territories of the GPi and striatum.

Multisynaptic inputs to the PMv from the limbic territory of the GPe and striatum

In the present study, we found that labeled neurons in the GPe were located mainly in the dorsoventrally middle portion at the caudal level and in the rostroventral portion. Many pioneer works reported that neurons in the former portion of the GPe responded to reaching or passive arm/wrist movements in monkeys (Iansek & Porter, 1980; DeLong *et al.*, 1985; Filion *et al.*, 1988; Hamada *et al.*, 1990; Yoshida *et al.*, 1993). Anatomical studies have revealed that this portion of the GPe receives inputs from the primary motor and premotor cortical areas via the striatum (Flaherty & Graybiel, 1993; Takada *et al.*, 1998b; Kaneda *et al.*, 2002; François *et al.*, 2004). Further, Grabli *et al.* (2004) have shown that the bicuculline (a GABA_A receptor antagonist) microinjection into this portion of the GPe induces abnormal movements. These observations indicate that this portion of the GPe corresponds to its motor territory.

Moreover, Grabli *et al.* (2004) have shown that microinjection of bicuculline into the rostroventral portion of the GPe of monkeys induces a stereotypic behavior, such as obsessively licking and biting fingers. Subsequently, by injecting an anterograde tracer into the same portion of the GPe, François *et al.* (2004) demonstrated that the

rostromedial portion of the GPe projected to the ventromedial portion of the SNr at its rostral level, which receives ample input from the ventral striatum, including the nucleus accumbens (Haber *et al.*, 1990, 1993, 2000). These findings indicate the rostromedial portion of the GPe corresponds to its limbic territory. In addition, a number of labeled neurons were distributed in the limbic territory of the striatum, including the ventromedial putamen and the nucleus accumbens. Previous studies reported the existence of neuronal labeling in the ventral striatum after rabies injection into the M1 (Kelly & Strick, 2004; Miyachi *et al.*, 2006) and the PMd (Saga *et al.*, 2011). This indicates that the ventral striatum sends diverse output projections to multiple motor cortical areas across synapses. Altogether, our findings have revealed that the PMv receives inputs from the limbic territories of the BG (i.e., the GPe and striatum). However, the exact pathways toward the PMv from the GPe and striatum still remain elusive. One potential candidate is the basal forebrain; it has been shown that the ventral striatum projects to the basal forebrain and cholinergic neurons therein in turn sends widespread outputs to the cerebral cortex (Kievit & Kuypers, 1975; Mesulam *et al.*, 1983; Haber *et al.*, 1993, 1995; Miyachi *et al.*, 2006). Actually, we found many

labeled neurons in the basal forebrain in our second-order samples. Further work is needed to address this issue.

Multisynaptic inputs to the PMv from the SNr and STN

We found the second-order labeled neurons in the SNr. A subset of labeled neurons was located in the central and dorsal portions of the SNr. These portions correspond to a sector that receives inputs from the M1- and/or SMA-recipient regions of the striatum (Haber *et al.*, 2000; Kaneda *et al.*, 2002). Furthermore, these portions have been shown to project to the PMd (Saga *et al.*, 2011), as well as to the prefrontal cortex (Middleton & Strick, 2002), across synapses. The overall findings suggest that the PMv may receive inputs from the primary and higher-order motor territories of the SNr.

Within the STN, we found that a subset of labeled neurons were located in the central to lateral portions within the caudal half of the nucleus. Previous studies have revealed that these portions of the STN correspond to the somatomotor territory (Nambu *et al.*, 1996, 1997; Inase *et al.*, 1999; Takada *et al.*, 2001; Kaneda *et al.*, 2002) that receives input from the M1 and sends output to the M1 across synapses. Further,

Nambu *et al.* (1996, 1997) showed that terminal labeling from the PMv, PMd, and SMA, as well as from the M1, was located in the same portions of the STN. Thus, the overall data indicate that the PMv receives inputs from the primary and higher-order motor territories of the STN. Another subset of labeled neurons was seen in the ventromedial portion of the rostral aspect of the nucleus. This portion of the rostral STN has been shown to correspond to the limbic territory (Haber *et al.*, 2000; Hamani *et al.*, 2004). By injecting an anterograde tracer into the ventromedial GPe, François *et al.* (2004) demonstrated that this GPe region projected to the ventromedial portion of the rostral STN. Altogether, neuronal labeling in the two distinct portions of the STN indicates that the PMv receives inputs from the primary/higher-order motor territories and the limbic territory of the STN.

Integration of diverse signals in the cortico-basal ganglia circuits

We have revealed that the cellular origins of multisynaptic projections from the BG to the PMv consist of two distinct motor territories, i.e., the primary and higher-order motor territories. Seminal studies have reported that the PMv is involved in spatial

attention (Kubota & Hamada, 1978; Rizzolatti *et al.*, 1981; Boussaoud & Wise, 1993a; Godschalk *et al.*, 1995) and reaching execution (Boussaoud & Wise, 1993b; Kurata & Hoshi, 2002; Schwartz *et al.*, 2004). Lesion studies in monkeys have supported these findings. The monkeys with hemi-ablation of the PMv resulted in deficits in orienting responses toward the contralateral space (Rizzolatti *et al.*, 1983; Scheiber, 2000). Similarly, microinjection of bicucullin into the dorsal GPe, including a portion from which the PMv receives input, induced attentional bias toward the contralateral space (Grabli *et al.*, 2004), and dopamine depletion in one side of the BG resulted in visual hemi-neglect (Apicella *et al.*, 1991; Miyashita *et al.*, 1995). Thus, the PMv may intensively interact with the BG for signal processing of spatial attention. In contrast, a subset of PMv neurons exhibits movement-related activity during reaching movement. Since the movement-related activity is most prominent in the M1 (Evarts, 1968; Georgopoulos *et al.*, 1982; Tanji & Kurata, 1982), the PMv may receive the information about the movement from the primary motor territory of the BG. In addition to spatial attention and movement execution, the PMv has been shown to participate in visuomotor transformation for reaching movement by encoding both visuospatial and

motor information (Boussaoud & Wise, 1993a, b; Kurata & Hoshi, 2002). Actually, inactivation of the PMv induced deficits in remapping from visual to motor space in shift-prism adaptation (Kurata & Hoshi, 1999). One intriguing possibility is that the PMv receives two distinct inputs concerning movement execution from the primary motor territory and spatial attention (or visual signals) from the higher-order motor territory of the BG, and that these two sets of information are integrated in the PMv to achieve the visuomotor transformation. After the motor commands are generated for the reaching movement, these signals may be transferred to the M1 via the intracortical connections between the PMv and the M1 (Dum & Strick, 2005; Dancause *et al.*, 2006) and via the circuits through the BG. In addition to the reaching movement, the PMv plays a crucial role in goal-directed grasping movements (Rizzolatti *et al.*, 1987). Inactivation of the PMv impairs grasping movements without any paralysis of finger movements *per se* (Fogassi *et al.*, 2001). Murata *et al.* (1997) have reported that PMv neurons reflect three-dimensional features of objects for grasping them. In the parietal and temporal cortical areas, object visual signals are amply represented in the inferior parietal lobule (IPL) and the inferotemporal cortex (IT). Of these the PMv is directly

interconnected with the IPL, but not with the IT (Luppino *et al.*, 2001; Rozzi *et al.*, 2006; Borra *et al.*, 2008). Anatomical studies have revealed that the IT projects to the IPL, suggesting that the PMv may receive input from the IT via the IPL. In addition, it has been reported that the IT projects not only to the caudate tail (Saint-Cyr *et al.*, 1990; Cheng *et al.*, 1997), but also to the lateral aspect of the caudate body (Webster *et al.*, 1993) in which we found the cellular origin of the projection to the PMv. Thus, the PMv may receive signals about the object shape represented in the IT via the BG. Taken together with the electrical stimulation and mapping studies (Gentilucci *et al.*, 1988; Godschalk *et al.*, 1995; Aflalo & Graziano, 2006; Maranesi *et al.*, 2012), these findings revealed a large overlap of zones representing reaching and grasping movements in the PMv. The overlap region may integrate movements with motor commands to achieve the visuomotor integration for grasping a target. An intriguing possibility is that the PMv-BG networks may be involved in the integration of the reaching and grasping components of forelimb movement (Gerbella *et al.*, 2015).

The motivational aspect, as well as the visual aspect, has been shown to influence action (Mogenson *et al.*, 1980; Haber *et al.*, 2000). In relation to this, it has been

revealed that the motor territory of the BG represents 'the vigor of movement'.

Inactivation of the caudoventral part of the GPi (i.e., the primary motor territory) resulted in the increase in the reaction time of a visually guided reaching task (Inase *et al.*, 1996a), the reduction in the movement velocity and the acceleration without impairment in reaching execution (Wenger *et al.*, 1999; Turner & Desmurget, 2010), and the undershoot toward motor targets (Turner & Anderson, 2005; Desmurget & Turner, 2008). These observations indicate that the motor territory of the BG already integrates the information concerning the visuospatial and motivational aspects. Thus, the PMv may receive the integrated 'vigor' signals from the motor territory of the BG (Turner & Desmurget, 2010). In addition to this, the limbic territory of the BG may provide the PMv with context-dependent motivational signals. Actually, Roesch and Olson (Roesch & Olson, 2004) showed that PMv neurons in macaque monkeys fired more strongly when the expected reward or penalty was larger, indicating that the PMv represents a general motivational signal of action. One intriguing possibility is that the PMv may receive it from the limbic territory of the BG. Altogether, it is likely that the PMv receives the information not only concerning the visual and motor aspects and

response vigor, but also about general motivation from the BG. Further, the motivational signal from the BG may enhance other types of forelimb movements in foraging behavior, such as locomotion, climbing, and reaching/grasping to eat food (Graziano, 2006; Rizzolatti *et al.*, 2014; Wise, 2006).

Comparison of the BG labeling after PMv and PMd injections

The PMd and PMv are suggested to play distinct roles in achievement of reaching and grasping movements. It has been shown that the PMd plays a major role in action planning based on multiple sets of sensory-motor association (i.e., indirect specification of action), whereas the PMv is involved more highly in matching actions directly with features (e.g., shape and location) of a target (i.e., direct guidance of action) (Hoshi & Tanji, 2007). In a prior report, we investigated the origins of multisynaptic inputs in the BG to the PMd (Saga *et al.*, 2011). By comparing the results obtained after the PMd and PMv injection, it was found that the number of labeled neurons in the output station of the BG (i.e., GPi and SNr) was comparable in the PMd and PMv injection cases, whereas those in the intermediate (i.e., GPe and STN) and input (i.e., striatum) stations

were higher in the PMv injection case than in the PMd injection case (Saga *et al.*, 2011).

These findings might suggest that the PMv is more tightly linked with the indirect

pathway (involving the GPe and STN) than the PMd, and that the greater degree of

funneling takes place in the striatum in the PMv-BG circuit than in the PMd-BG circuit.

However, such notions should be taken as a preliminary account because the subjects,

injection volumes, and viral lots differ in the PMd and PMv injections. To better

characterize possible differences in the network architecture of the PMv-BG and

PMd-BG circuits, it is needed to overcome these technical issues.

Acknowledgements

We thank T. Ogata and T. Kuroda for technical assistance. This work was supported by

CREST, JST (E. H. and M. T.), and a Grant-in Aid for Young Scientists KAKENHI

70728162 (H. I.) from Japan Society for Promotion of Science.

Abbreviations [alphabetic order]

Anterior commissure (ac), Basal ganglia (BG), Dorsal premotor cortex (PMd), Globus

pallidus external segment (GPe), Globus pallidus internal segment (GPi), Primary motor cortex (M1), Substantia nigra pars reticulata (SNr), Subthalamic nucleus (STN), Supplementary motor cortex (SMA), Ventral premotor cortex (PMv)

References

- Aflalo, T.N. & Graziano, M.S.A. (2006) Possible origins of the complex topographic organization of motor cortex: Reduction of a multidimensional space onto a two-dimensional array. *J. Neurosci.*, **26**, 6288–6297.
- Akkal, D., Dum, R.P., & Strick, P.L. (2007) Supplementary motor area and presupplementary motor area: targets of basal ganglia and cerebellar output. *J. Neurosci.*, **27**, 10659–10673.
- Alexander, G.E. & Crutcher, M.D. (1990) Functional architecture of basal ganglia circuits: neural substrates of parallel processing. *Trends Neurosci.*, **13**, 266–271.
- Apicella, P., Legallet, E., Nieoullon, A., & Trouche, E. (1991) Neglect of contralateral visual stimuli in monkeys with unilateral striatal dopamine depletion. *Behav. Brain Res.*, **46**, 187–195.
- Barbas, H. & Pandya, D.N. (1987) Architecture and frontal cortical connections of the premotor cortex (area 6) in the rhesus monkey. *J. Comp. Neurol.*, **256**, 211–228.
- Barbas, H., & García-Cabezas, M. Á. (2015). Motor cortex layer 4: less is more. *Trends in Neurosci.*, **38**, 259–261.
- Borra, E., Belmalih, A., Calzavara, R., Gerbella, M., Murata, A., Rozzi, S., & Luppino, G. (2008) Cortical connections of the macaque anterior intraparietal (AIP) area. *Cereb. Cortex*, **18**, 1094–1111.
- Boussaoud, D. & Wise, S.P. (1993a) Primate frontal cortex: neuronal activity following attentional versus intentional cues. *Exp. Brain Res.*, **95**, 15–27.
- Boussaoud, D. & Wise, S.P. (1993b) Primate frontal cortex: effects of stimulus and movement. *Exp. Brain Res.*, **95**, 28–40.

- Caminiti, R., Johnson, P.B., Galli, C., Ferraina, S., & Burnod, Y. (1991) Making arm movements within different parts of space: the premotor and motor cortical representation of a coordinate system for reaching to visual targets. *J. Neurosci.*, **11**, 1182–1197.
- Cheng, K., Saleem, K.S., & Tanaka, K. (1997) Organization of corticostriatal and corticoamygdalar projections arising from the anterior inferotemporal area TE of the macaque monkey: a Phaseolus vulgaris leucoagglutinin study. *J. Neurosci.*, **17**, 7902–7925.
- Dancause, N., Barbay, S., Frost, S.B., Plautz, E.J., Popescu, M., Dixon, P.M., Stowe, A.M., Friel, K.M., & Nudo, R.J. (2006) Topographically divergent and convergent connectivity between premotor and primary motor cortex. *Cereb. Cortex*, **16**, 1057–1068.
- DeLong, M.R., Crutcher, M.D., & Georgopoulos, A.P. (1985) Primate globus pallidus and subthalamic nucleus: functional organization. *J. Neurophysiol.*, **53**, 530–543.
- Desmurget, M. & Turner, R.S. (2008) Testing basal ganglia motor functions through reversible inactivations in the posterior internal globus pallidus. *J. Neurophysiol.*, **99**, 1057–1076.
- Dum, R.P. & Strick, P.L. (2005) Frontal lobe inputs to the digit representations of the motor areas on the lateral surface of the hemisphere. *J. Neurosci.*, **25**, 1375–1386.
- Evarts, E.V. (1968) Relation of pyramidal tract activity to force exerted during voluntary movement. *J. Neurophysiol.*, **31**, 14–27.
- Filion, M., Tremblay, L., & Bédard, P.J. (1988) Abnormal influences of passive limb movement on the activity of globus pallidus neurons in parkinsonian monkeys. *Brain Res.*, **444**, 165–176.
- Flaherty, A.W. & Graybiel, A.M. (1993) Two input systems for body representations in the primate striatal matrix: experimental evidence in the squirrel monkey. *J. Neurosci.*, **13**, 1120–1137.
- Fogassi, L., Gallese, V., Buccino, G., Craighero, L., Fadiga, L., & Rizzolatti, G. (2001) Cortical mechanism for the visual guidance of hand grasping movements in the monkey: A reversible inactivation study. *Brain*, **124**, 571–586.
- François, C., Grabli, D., McCairn, K., Jan, C., Karachi, C., Hirsch, E.-C., Féger, J., & Tremblay, L. (2004) Behavioural disorders induced by external globus pallidus dysfunction in primates II. Anatomical study. *Brain*, **127**, 2055–2070.

- García-Cabezas, M. Á., & Barbas, H. (2014). Area 4 has layer IV in adult primates. *Eur. J. Neurosci.*, **39**, 1824–1834.
- Gentilucci, M., Fogassi, L., Luppino, G., Matelli, M., Camarda, R., & Rizzolatti, G. (1988) Functional organization of inferior area 6 in the macaque monkey. *Exp. Brain Res.*, **71**, 475–490.
- Georgopoulos, A.P., Kalaska, J.F., Caminiti, R., & Massey, J.T. (1982) On the relations between the direction of two-dimensional arm movements and cell discharge in primate motor cortex. *J. Neurosci.*, **2**, 1527–1537.
- Gerbella, M., Borra, E., Mangiaracina, C., Rozzi, S., & Luppino, G. (2015) Corticostriate Projections from Areas of the “Lateral Grasping Network”: Evidence for Multiple Hand-Related Input Channels. *Cereb. Cortex*, (in press).
- Godschalk, M., Mitz, A.R., van Duin, B., & van der Burg, H. (1995) Somatotopy of monkey premotor cortex examined with microstimulation. *Neurosci. Res.*, **23**, 269–279.
- Grabli, D., McCairn, K., Hirsch, E.-C., Agid, Y., Féger, J., François, C., & Tremblay, L. (2004) Behavioural disorders induced by external globus pallidus dysfunction in primates: I. Behavioural study. *Brain*, **127**, 2039–2054.
- Graziano, M. (2006) The organization of behavioral repertoire in motor cortex. *Annu. Rev. Neurosci.*, **29**, 105–134.
- Haber, S.N., Fudge, J.L., & McFarland, N.R. (2000) Striatonigrostriatal pathways in primates form an ascending spiral from the shell to the dorsolateral striatum. *J. Neurosci.*, **20**, 2369–2382.
- Haber, S.N., Kunishio, K., Mizobuchi, M., & Lynd-Balta, E. (1995) The orbital and medial prefrontal circuit through the primate basal ganglia. *J. Neurosci.*, **15**, 4851–4867.
- Haber, S.N., Lynd, E., Klein, C., & Groenewegen, H.J. (1990) Topographic organization of the ventral striatal efferent projections in the rhesus monkey: An anterograde tracing study. *J. Comp. Neurol.*, **293**, 282–298.
- Haber, S.N., Lynd-Balta, E., & Mitchell, S.J. (1993) The organization of the descending ventral pallidal projections in the monkey. *J. Comp. Neurol.*, **329**, 111–128.
- Halsband, U. & Passingham, R.E. (1985) Premotor cortex and the conditions for movement in monkeys (Macaca fascicularis). *Behav. Brain Res.*, **18**, 269–277.

- Hamada, I., DeLong, M.R., & Mano, N. (1990) Activity of identified wrist-related pallidal neurons during step and ramp wrist movements in the monkey. *J. Neurophysiol.*, **64**, 1892–1906.
- Hamani, C., Saint-Cyr, J.A., Fraser, J., Kaplitt, M., & Lozano, A.M. (2004) The subthalamic nucleus in the context of movement disorders. *Brain*, **127**, 4–20.
- Hashimoto, M., Takahara, D., Hirata, Y., Inoue, K.-I., Miyachi, S., Nambu, A., Tanji, J., Takada, M., & Hoshi, E. (2010) Motor and non-motor projections from the cerebellum to rostrocaudally distinct sectors of the dorsal premotor cortex in macaques. *Eur. J. Neurosci.*, **31**, 1402–1413.
- Hoover, J.E. & Strick, P.L. (1993) Multiple output channels in the basal ganglia. *Science*, **259**, 819–821.
- Hoover, J.E. & Strick, P.L. (1999) The organization of cerebellar and basal ganglia outputs to primary motor cortex as revealed by retrograde transneuronal transport of herpes simplex virus type 1. *J. Neurosci.*, **19**, 1446–1463.
- Hoshi, E. & Tanji, J. (2000) Integration of target and body-part information in the premotor cortex when planning action. *Nature*, **408**, 466–470.
- Hoshi, E. & Tanji, J. (2006) Differential involvement of neurons in the dorsal and ventral premotor cortex during processing of visual signals for action planning. *J. Neurophysiol.*, **95**, 3596–3616.
- Hoshi, E. & Tanji, J. (2007) Distinctions between dorsal and ventral premotor areas: anatomical connectivity and functional properties. *Curr. Opin. Neurobiol.*, **17**, 234–242.
- Iansek, R. & Porter, R. (1980) The monkey globus pallidus: neuronal discharge properties in relation to movement. *J. Physiol.*, **301**, 439–455.
- Inase, M., Buford, J.A., & Anderson, M.E. (1996a) Changes in the control of arm position, movement, and thalamic discharge during local inactivation in the globus pallidus of the monkey. *J. Neurophysiol.*, **75**, 1087–1104.
- Inase, M., Sakai, S.T., & Tanji, J. (1996b) Overlapping corticostriatal projections from the supplementary motor area and the primary motor cortex in the macaque monkey: an anterograde double labeling study. *J. Comp. Neurol.*, **373**, 283–296.
- Inase, M., Tokuno, H., Nambu, A., Akazawa, T., & Takada, M. (1999) Corticostriatal and corticosubthalamic input zones from the presupplementary motor area in the

- macaque monkey: comparison with the input zones from the supplementary motor area. *Brain Res.*, **833**, 191–201.
- Kalaska, J.F. & Crammond, D.J. (1992) Cerebral cortical mechanisms of reaching movements. *Science*, **255**, 1517–1523.
- Kaneda, K., Nambu, A., Tokuno, H., & Takada, M. (2002) Differential processing patterns of motor information via striatopallidal and striatonigral projections. *J. Neurophysiol.*, **88**, 1420–1432.
- Kelly, R.M. & Strick, P.L. (2004) Macro-architecture of basal ganglia loops with the cerebral cortex: use of rabies virus to reveal multisynaptic circuits. *Prog. Brain Res.*, **143**, 449–459.
- Kievit, J. & Kuypers, H.G. (1975) Basal forebrain and hypothalamic connection to frontal and parietal cortex in the Rhesus monkey. *Science*, **187**, 660–662.
- Kubota, K. & Hamada, I. (1978) Visual tracking and neuron activity in the post-arcuate area in monkeys. *J. Physiol. (Paris)*, **74**, 297–312.
- Kurata, K. & Wise, S.P. (1988) Premotor cortex of rhesus monkeys: set-related activity during two conditional motor tasks. *Exp. Brain Res.*, **69**, 327–343.
- Kurata, K. (1993) Premotor cortex of monkeys: set-and movement-related activity reflecting amplitude and direction of wrist movements. *J. Neurophysiol.*, **69**, 187–187.
- Kurata, K. & Hoffman, D.S. (1994) Differential effects of muscimol microinjection into dorsal and ventral aspects of the premotor cortex of monkeys. *J. Neurophysiol.*, **71**, 1151–1164.
- Kurata, K. & Hoshi, E. (1999) Reacquisition deficits in prism adaptation after muscimol microinjection into the ventral premotor cortex of monkeys. *J. Neurophysiol.*, **81**, 1927–1938.
- Kurata, K. & Hoshi, E. (2002) Movement-related neuronal activity reflecting the transformation of coordinates in the ventral premotor cortex of monkeys. *J. Neurophysiol.*, **88**, 3118–3132.
- Luppino, G., Calzavara, R., Rozzi, S., & Matelli, M. (2001) Projections from the superior temporal sulcus to the agranular frontal cortex in the macaque. *Eur. J. Neurosci.*, **14**, 1035–1040.

- Luppino, G., Murata, A., Govoni, P., & Matelli, M. (1999) Largely segregated parietofrontal connections linking rostral intraparietal cortex (areas AIP and VIP) and the ventral premotor cortex (areas F5 and F4). *Exp. Brain Res.*, **128**, 181–187.
- Maranesi, M., Rodà, F., Bonini, L., Rozzi, S., Ferrari, P.F., Fogassi, L., & Coudé, G. (2012) Anatomic-functional organization of the ventral primary motor and premotor cortex in the macaque monkey. *Eur. J. Neurosci.*, **36**, 3376–3387.
- Matelli, M., Camarda, R., Glickstein, M., & Rizzolatti, G. (1986) Afferent and efferent projections of the inferior area 6 in the macaque monkey. *J. Comp. Neurol.*, **251**, 281–298.
- Matelli, M., Govoni, P., Galletti, C., Kutz, D.F., & Luppino, G. (1998) Superior area 6 afferents from the superior parietal lobule in the macaque monkey. *J. Comp. Neurol.*, **402**, 327–352.
- Matelli, M., Luppino, G., & Rizzolatti, G. (1985) Patterns of cytochrome oxidase activity in the frontal agranular cortex of the macaque monkey. *Behav. Brain Res.*, **18**, 125–136.
- Mesulam, M.M., Mufson, E.J., Levey, A.I., & Wainer, B.H. (1983) Cholinergic innervation of cortex by the basal forebrain: cytochemistry and cortical connections of the septal area, diagonal band nuclei, nucleus basalis (substantia innominata), and hypothalamus in the rhesus monkey. *J. Comp. Neurol.*, **214**, 170–197.
- Middleton, F.A. & Strick, P.L. (2002) Basal-ganglia “projections” to the prefrontal cortex of the primate. *Cereb. Cortex*, **12**, 926–935.
- Miyachi, S., Lu, X., Imanishi, M., Sawada, K., Nambu, A., & Takada, M. (2006) Somatotopically arranged inputs from putamen and subthalamic nucleus to primary motor cortex. *Neurosci. Res.*, **56**, 300–308.
- Miyashita, N., Hikosaka, O., & Kato, M. (1995) Visual hemineglect induced by unilateral striatal dopamine deficiency in monkeys. *Neuroreport*, **6**, 1257–1260.
- Mogenson, G.J., Jones, D.L., & Yim, C.Y. (1980) From motivation to action: functional interface between the limbic system and the motor system. *Prog. Neurobiol.*, **14**, 69–97.
- Morel, A., Liu, J., Wannier, T., Jeanmonod, D., & Rouiller, E.M. (2005) Divergence and convergence of thalamocortical projections to premotor and supplementary motor cortex: a multiple tracing study in the macaque monkey. *Eur. J. Neurosci.*, **21**, 1007–1029.

- Murata, A., Fadiga, L., Fogassi, L., Gallese, V., Raos, V., & Rizzolatti, G. (1997) Object representation in the ventral premotor cortex (area F5) of the monkey. *J. Neurophysiol.*, **78**, 2226–2230.
- Nambu, A., Takada, M., Inase, M., & Tokuno, H. (1996) Dual somatotopical representations in the primate subthalamic nucleus: evidence for ordered but reversed body-map transformations from the primary motor cortex and the supplementary motor area. *J. Neurosci.*, **16**, 2671–2683.
- Nambu, A., Tokuno, H., Inase, M., & Takada, M. (1997) Corticosubthalamic input zones from forelimb representations of the dorsal and ventral divisions of the premotor cortex in the macaque monkey: comparison with the input zones from the primary motor cortex and the supplementary motor area. *Neurosci. Lett.*, **239**, 13–16.
- Petrides, M. & Pandya, D.N. (1999) Dorsolateral prefrontal cortex: comparative cytoarchitectonic analysis in the human and the macaque brain and corticocortical connection patterns. *Eur. J. Neurosci.*, **11**, 1011–1036.
- Parent, A. & Hazrati, L.-N. (1995a) Functional anatomy of the basal ganglia. I. The cortico-basal ganglia-thalamo-cortical loop. *Brain Res. Rev.*, **20**, 91–127.
- Parent, A. & Hazrati, L.-N. (1995b) Functional anatomy of the basal ganglia. II. The place of subthalamic nucleus and external pallidum in basal ganglia circuitry. *Brain Res. Rev.*, **20**, 128–154.
- Raos, V., Franchi, G., Gallese, V., & Fogassi, L. (2003) Somatotopic organization of the lateral part of area F2 (dorsal premotor cortex) of the macaque monkey. *J. Neurophysiol.*, **89**, 1503–1518.
- Raos, V., Umiltà, M.A., Gallese, V., & Fogassi, L. (2004) Functional properties of grasping-related neurons in the dorsal premotor area F2 of the macaque monkey. *J. Neurophysiol.*, **92**, 1990–2002.
- Raos, V., Umiltà, M.A., Murata, A., Fogassi, L., & Gallese, V. (2006) Functional properties of grasping-related neurons in the ventral premotor area F5 of the macaque monkey. *J. Neurophysiol.*, **95**, 709–729.
- Rizzolatti, G., Cattaneo, L., Fabbri-Destro, M., & Rozzi, S. (2014) Cortical mechanisms underlying the organization of goal-directed actions and mirror neuron-based action understanding. *Physiol. Rev.*, **94**, 655–706.

- Rizzolatti, G., Gentilucci, M., Fogassi, L., Luppino, G., Matelli, M., & Ponzoni-Maggi, S. (1987) Neurons related to goal-directed motor acts in inferior area 6 of the macaque monkey. *Exp. Brain Res.*, **67**, 220–224.
- Rizzolatti, G., Luppino, G., & Matelli, M. (1998) The organization of the cortical motor system: new concepts. *Electroencephalogr Clin. Neurophysiol.*, **106**, 283–296.
- Rizzolatti, G., Matelli, M., & Pavesi, G. (1983) Deficits in attention and movement following the removal of postarcuate (area 6) and prearcuate (area 8) cortex in macaque monkeys. *Brain*, **106 (Pt 3)**, 655–673.
- Rizzolatti, G., Scandolara, C., Matelli, M., & Gentilucci, M. (1981) Afferent properties of periarculate neurons in macaque monkeys. II. Visual responses. *Behav. Brain Res.*, **2**, 147–163.
- Roesch, M.R. & Olson, C.R. (2004) Neuronal activity related to reward value and motivation in primate frontal cortex. *Science*, **304**, 307–310.
- Rozzi, S., Calzavara, R., Belmalih, A., Borra, E., Gregoriou, G.G., Matelli, M., & Luppino, G. (2006) Cortical connections of the inferior parietal cortical convexity of the macaque monkey. *Cereb. Cortex*, **16**, 1389–1417.
- Saga, Y., Hirata, Y., Takahara, D., Inoue, K.-I., Miyachi, S., Nambu, A., Tanji, J., Takada, M., & Hoshi, E. (2011) Origins of multisynaptic projections from the basal ganglia to rostrocaudally distinct sectors of the dorsal premotor area in macaques. *Eur. J. Neurosci.*, **33**, 285–297.
- Saint-Cyr, J.A., Ungerleider, L.G., & Desimone, R. (1990) Organization of visual cortical inputs to the striatum and subsequent outputs to the pallido-nigral complex in the monkey. *J. Comp. Neurol.*, **298**, 129–156.
- Schieber, M.H. (2000) Inactivation of the ventral premotor cortex biases the laterality of motoric choices. *Exp. Brain Res.*, **130**, 497–507.
- Schwartz, A.B., Moran, D.W., & Reina, G.A. (2004) Differential representation of perception and action in the frontal cortex. *Science*, **303**, 380–383.
- Scott, S.H., Sergio, L.E., & Kalaska, J.F. (1997) Reaching movements with similar hand paths but different arm orientations. II. activity of individual cells in dorsal premotor cortex and parietal area 5. *J. Neurophysiol.*, **78**, 2413–2426.
- Takada, M., Tokuno, H., Hamada, I., Inase, M., Ito, Y., Imanishi, M., Hasegawa, N., Akazawa, T., Hatanaka, N., & Nambu, A. (2001) Organization of inputs from

- cingulate motor areas to basal ganglia in macaque monkey. *Eur. J. Neurosci.*, **14**, 1633–1650.
- Takada, M., Tokuno, H., Nambu, A., & Inase, M. (1998a) Corticostriatal input zones from the supplementary motor area overlap those from the contra- rather than ipsilateral primary motor cortex. *Brain Res.*, **791**, 335–340.
- Takada, M., Tokuno, H., Nambu, A., & Inase, M. (1998b) Corticostriatal projections from the somatic motor areas of the frontal cortex in the macaque monkey: segregation versus overlap of input zones from the primary motor cortex, the supplementary motor area, and the premotor cortex. *Exp. Brain Res.*, **120**, 114–128.
- Takahara, D., Inoue, K.-I., Hirata, Y., Miyachi, S., Nambu, A., Takada, M., & Hoshi, E. (2012) Multisynaptic projections from the ventrolateral prefrontal cortex to the dorsal premotor cortex in macaques - anatomical substrate for conditional visuomotor behavior. *Eur. J. Neurosci.*, **36**, 3365–3375.
- Tanji, J. & Kurata, K. (1982) Comparison of movement-related activity in two cortical motor areas of primates. *J. Neurophysiol.*, **48**, 633–653.
- Turner, R.S. & Anderson, M.E. (2005) Context-dependent modulation of movement-related discharge in the primate globus pallidus. *J. Neurosci.*, **25**, 2965–2976.
- Turner, R.S. & Desmurget, M. (2010) Basal ganglia contributions to motor control: a vigorous tutor. *Curr. Opin. Neurobiol.*, **20**, 704–716.
- Umiltà, M.A., Brochier, T., Spinks, R.L., & Lemon, R.N. (2007) Simultaneous recording of macaque premotor and primary motor cortex neuronal populations reveals different functional contributions to visuomotor grasp. *J. Neurophysiol.*, **98**, 488–501.
- Webster, M.J., Bachevalier, J., & Ungerleider, L.G. (1993) Subcortical connections of inferior temporal areas TE and TEO in macaque monkeys. *J. Comp. Neurol.*, **335**, 73–91.
- Wenger, K.K., Musch, K.L., & Mink, J.W. (1999) Impaired reaching and grasping after focal inactivation of globus pallidus pars interna in the monkey. *J. Neurophysiol.*, **82**, 2049–2060.
- Wise, S.P. (1985) The primate premotor cortex: past, present, and preparatory. *Annu. Rev. Neurosci.*, **8**, 1–19.

- Wise, S.P. (2006) The ventral premotor cortex, corticospinal region C, and the origin of primates. *Cortex*, **42**, 521–524.
- Wise, S.P., Boussaoud, D., Johnson, P.B., & Caminiti, R. (1997) Premotor and parietal cortex: corticocortical connectivity and combinatorial computations. *Annu. Rev. Neurosci.*, **20**, 25–42.
- Yamagata, T., Nakayama, Y., Tanji, J., & Hoshi, E. (2009) Processing of visual signals for direct specification of motor targets and for conceptual representation of action targets in the dorsal and ventral premotor cortex. *J. Neurophysiol.*, **102**, 3280–3294.
- Yamawaki, N., Borges, K., Suter, B. A., Harris, K. D., & Shepherd, G. M. G. (2014). A genuine layer 4 in motor cortex with prototypical synaptic circuit connectivity. *eLife*, **3**, e05422.
- Yoshida, S., Nambu, A., & Jinnai, K. (1993) The distribution of the globus pallidus neurons with input from various cortical areas in the monkeys. *Brain Res.*, **611**, 170–174.
- Zemanick, M.C., Strick, P.L., & Dix, R.D. (1991) Direction of transneuronal transport of herpes simplex virus 1 in the primate motor system is strain-dependent. *Proc. Natl. Acad. Sci. USA*, **88**, 8048–8051.

Table 1.
Summary of experiments

Monkey	Species	Injection site	Tracer	Survival (days)	Injection tracks (n)	Injection volume (μ L)
Case 1	<i>M. fuscata</i>	PMv	CSV-11	3	2	2.0
Case 2	<i>M. fuscata</i>	PMv	CSV-11	3	2	2.0
Case 3	<i>M. fuscata</i>	PMv	CSV-11	4	2	2.0
Case 4	<i>M. fuscata</i>	PMv	CSV-11	4	2	2.0

Figure Legends

Figure 1

Locations of injection sites in the PMv. (A) Diagram illustrating the frontal lobe of the macaque monkey. The rectangular area drawn with broken line is enlarged in (B). (B) Schematic view of injection site of rabies virus in the PMv. The circle drawn with the dotted line indicates the intended injection site. Within the intended injection site, the small gray circles (0.5 mm in radius) indicate the estimated viral spread around the injection tracks. The genu of the arcuate sulcus (AS) is denoted with the asterisk. The border between the premotor cortex and the primary motor cortex (M1) is represented by the broken line. (C) Drawing illustrating a slice with an injection track for each case. In (C-E), an arrowhead points to an injection track. (D) Low-magnification microphotograph of a Nissl-stained section of Case 1. (E) Low-magnification microphotograph of the injection site in Case 1 three days after rabies injection. In the low-power image, labeled neurons are densely distributed around the injection site. (F) The boxed region in the panel (D) is enlarged. Many neurons are seen to be labeled in a Golgi-like manner. CS, central sulcus; PS, principal sulcus; AS, the arcuate sulcus; Spur,

spur of AS; Spur, spur of AS; Cg, cingulate sulcus. Scale bars in (D) and (E): 500 μ m.

Scale bar in (F): 50 μ m.

Figure 2

Neuronal labeling in the GP and SNr. (A and B) Second-order neuron labeling in the GPi (A) and the SNr (B) 3 days after the rabies injection into the PMv. (C) Third-order neuron labeling in the GPe 4 days after the rabies injection. The boxed region in each panel is enlarged in each microphotograph. Scale bars in A-C: 50 μ m. oGPi, outer portion of GPi; iGPi, inner portion of GPi; SNc, substantia nigra compacta; SNr, substantia nigra reticulata.

Figure 3

Summary plot of the number of labeled neuron. Mean values of the labeled neurons in each nucleus are shown. Each data point at the top of each bar indicates the number of labeled neuron in each case (Case 1, filled circle; Case 2, open circle; Case 3, filled square; Case 4, open square). The distance between the data point and the mean

corresponds to standard error of the mean. White bars indicate mean values of labeled neurons (second-order neurons) observed in the GPi and SNr, while gray bars indicate the mean values of the labeled neurons (third-order neurons) observed in the GPe, STN and striatum (Cd and Put). Cd, caudate nucleus; GPe, external segment of the globus pallidus; GPi, internal segment of the globus pallidus; Put, putamen; SNr, substantia nigra pars reticulata; SNT, subthalamic nucleus.

Figure 4

Distribution of labeled neurons in the GPi. Six coronal sections are arranged rostrocaudally from the left to right (A-F, A'-F'). Each row represents data from a single subject (Cases 1, 2). Each dot indicates the location of an infected neuron labeled by retrograde transneuronal transport (second-order neurons). The border between the oGPi and the iGPi is represented with the dotted line. Scale bar: 1 mm. oGPi, outer portion of GPi; iGPi, inner portion of GPi.

Figure 5

Density maps of GPi neurons labeled after rabies virus injections into the PMv. (A and B) Procedures to construct two-dimensional density maps of the GPi. The unfolding process started with drawing a line through the border between the outer (oGPi) and inner (iGPi) portions of the GPi. The reference points were placed at the bottom (the red circle) and the top (the blue circle) of the GPi. The position of each labeled neuron was projected onto the line. Then, each line through the nucleus was aligned on the ventral edge of the GPi (B). Neurons were divided into $300 \times 300 \mu\text{m}^2$ bins. (C and D) Density maps of the GPi neuron labeling in each case. The number of labeled neurons in each bin was counted and color-coded.

Figure 6

Distribution of labeled neurons in the SNr. Six coronal sections are arranged rostrocaudally from the left to right (A-F, A'-F'). Each row represents data from a single subject (Cases 1, 2). Each dot indicates the location of an infected neuron labeled by retrograde transneuronal transport (second-order neurons). The number in each section indicates its relative rostrocaudal position within the SNr (most rostral level = 0, most

caudal level = 1). The lines in each section indicate the border between the SNr and the substantia nigra pars compacta (SNc).

Figure 7

Distribution of labeled neurons in the GPe (third-order neurons) and the GPi (second-order or third-order neurons). Six coronal sections are arranged rostrocaudally from the left to right (A-F, A'-F'). Each row represents data from a single subject (Cases 3, 4). Each dot indicates the location of an infected neuron.

Figure 8

Density maps of GPe neurons labeled after PMv injections. (A and B) Procedures to construct two-dimensional density maps of the GPe. The unfolding process started with drawing line through the center of the GPe. The reference points were placed at the bottom (the red circle) and at the top (the blue circle) of the GPe. The position of each labeled neuron was projected onto the central line. Then, each line through the nucleus was aligned on the ventral edge of the GPe (B). Neurons were divided into $300 \times$

300 μm^2 bins. (C, D) Density maps of the GPe neuron labeling in each case. The number of labeled neurons in each bin was counted and color-coded.

Figure 9

Distribution of labeled neurons in the STN. Six coronal sections are arranged rostrocaudally from the left to right (A-F, A'-F'). Each row represents data from a single subject (Cases 3, 4).

Figure 10

Distribution of labeled neurons in the striatum. Six coronal sections are arranged rostrocaudally from the left to right (A-F, A'-F'). Each row represents data from a single subject (Cases 3, 4). For each section, the AP (anterior-posterior) level relative to ac (anterior commissure) is indicated in mm. Scale bar in F' applies to all panels (A-F, A'-F').

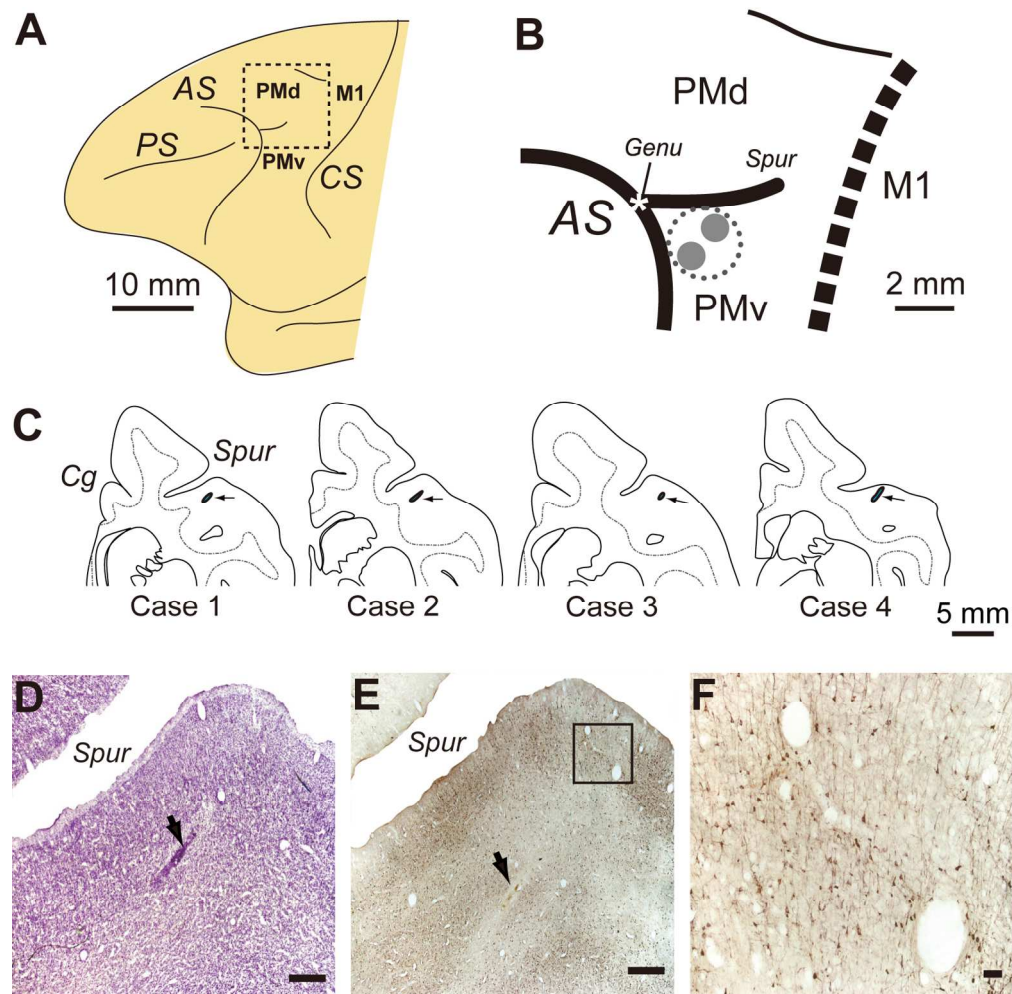


Figure 1
144x143mm (300 x 300 DPI)

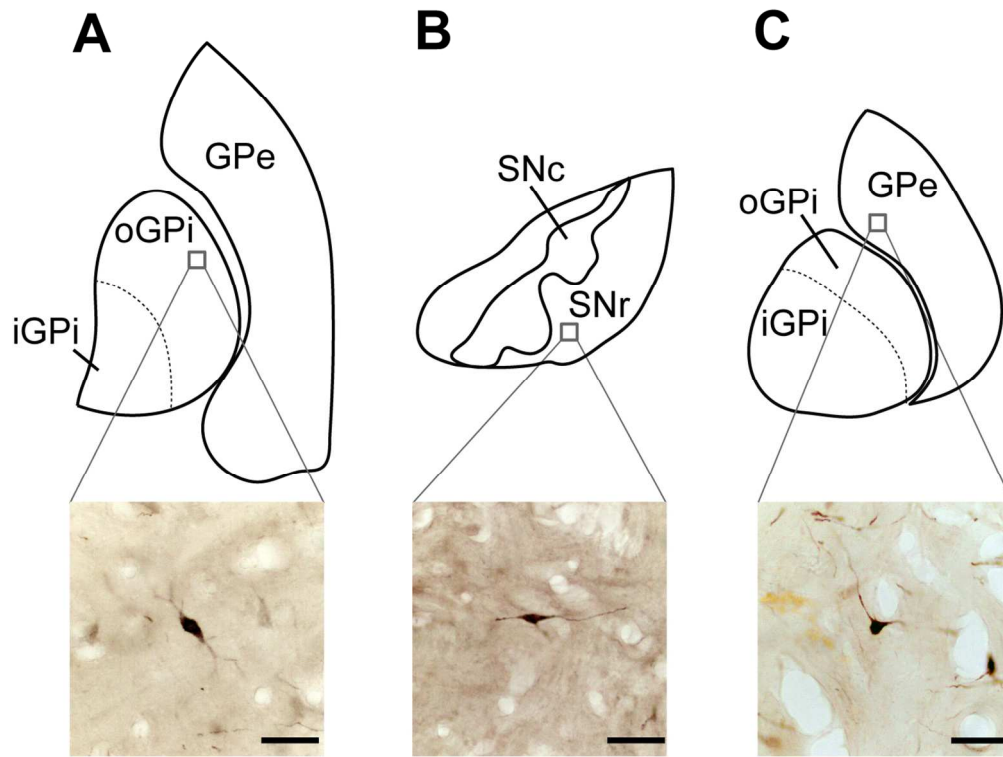


Figure 2
118x88mm (300 x 300 DPI)

review

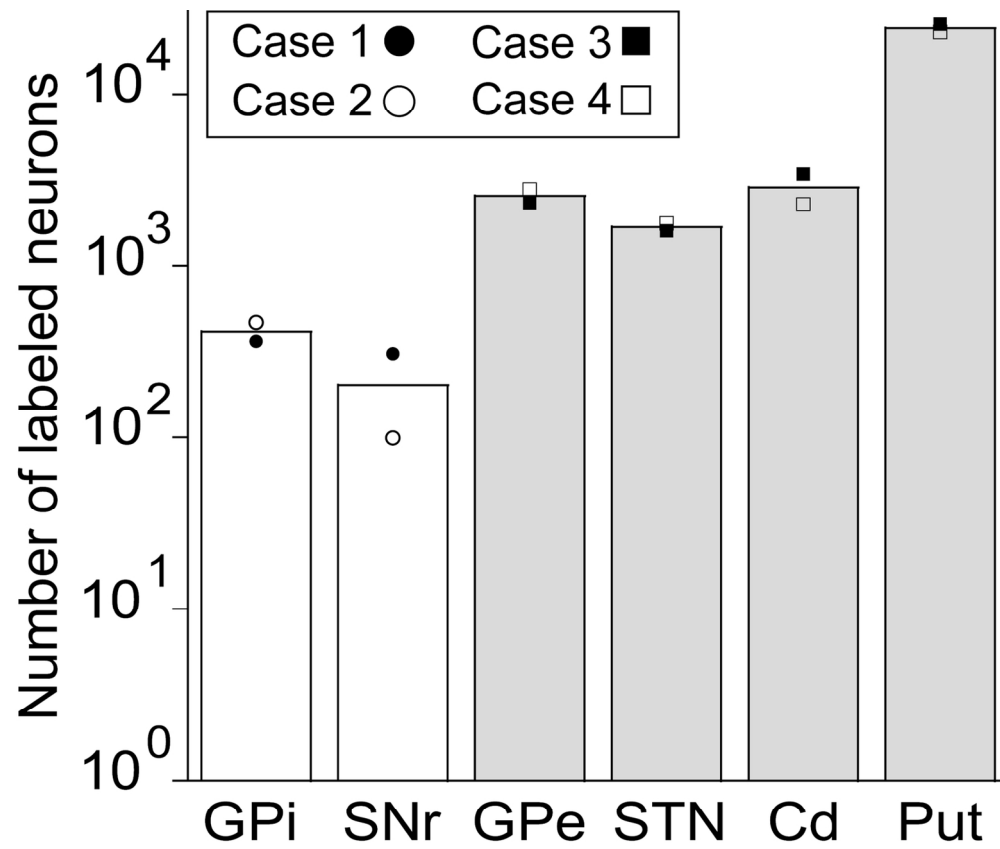


Figure 3
70x63mm (600 x 600 DPI)

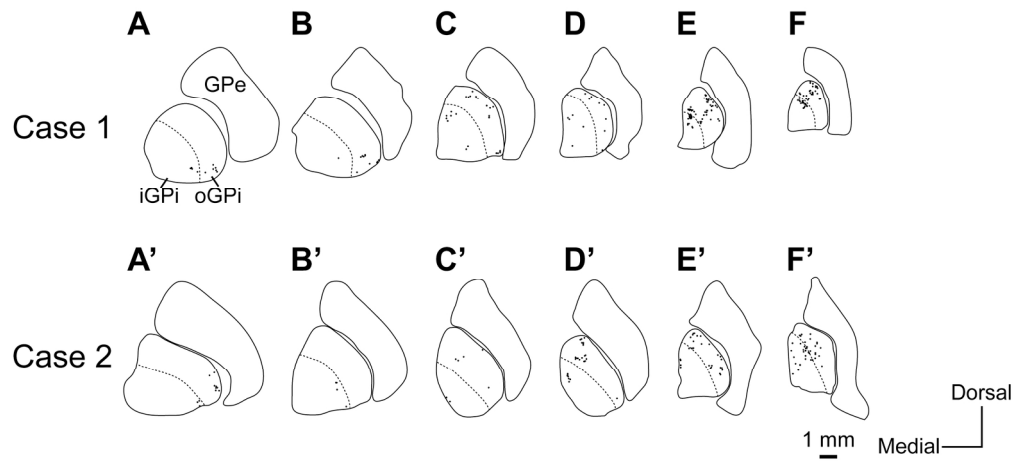


Figure 4
90x40mm (600 x 600 DPI)

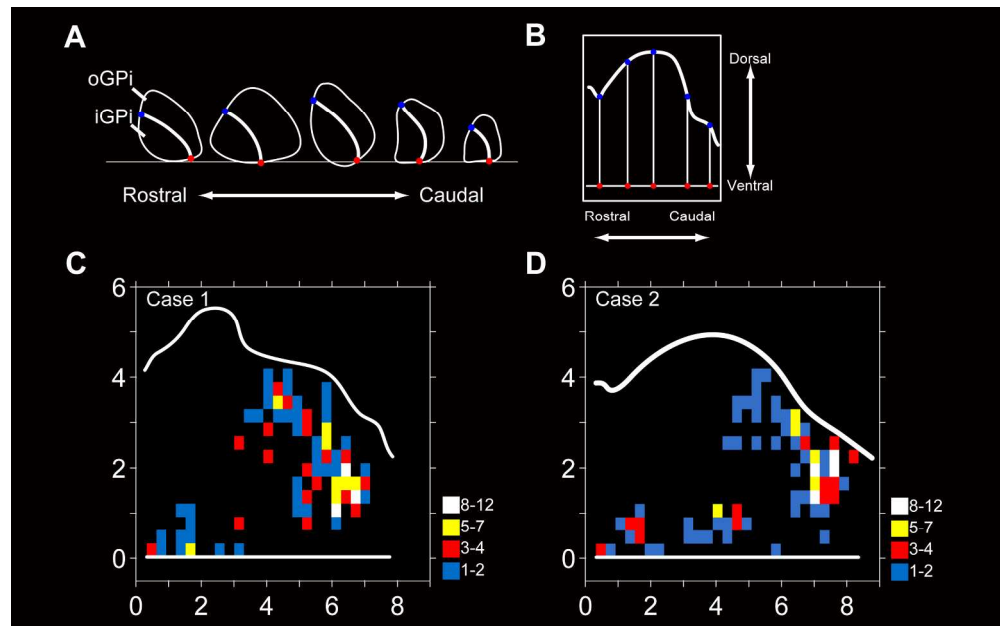


Figure 5
208x129mm (300 x 300 DPI)

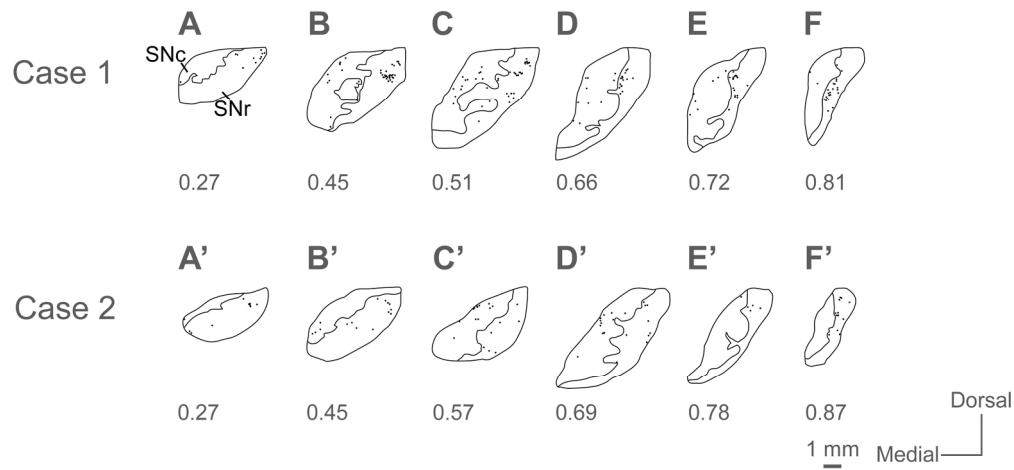


Figure 6
90x41mm (600 x 600 DPI)

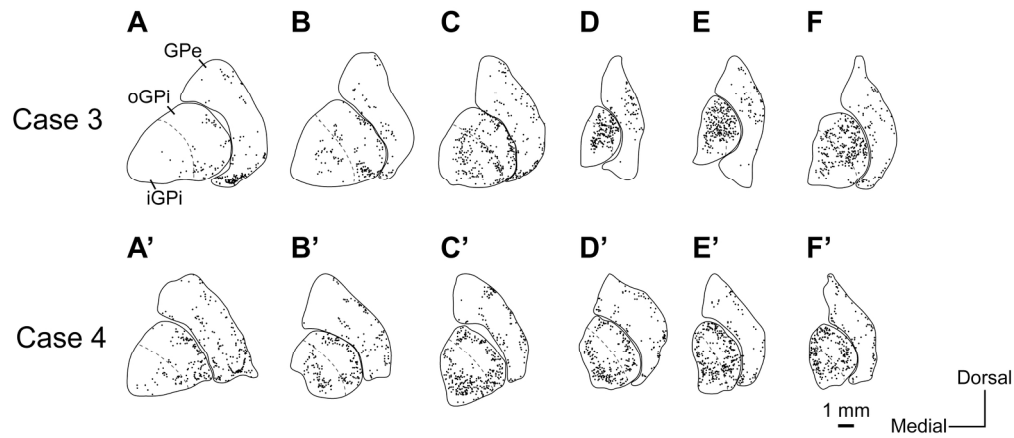


Figure 7
95x40mm (600 x 600 DPI)

Peer Review

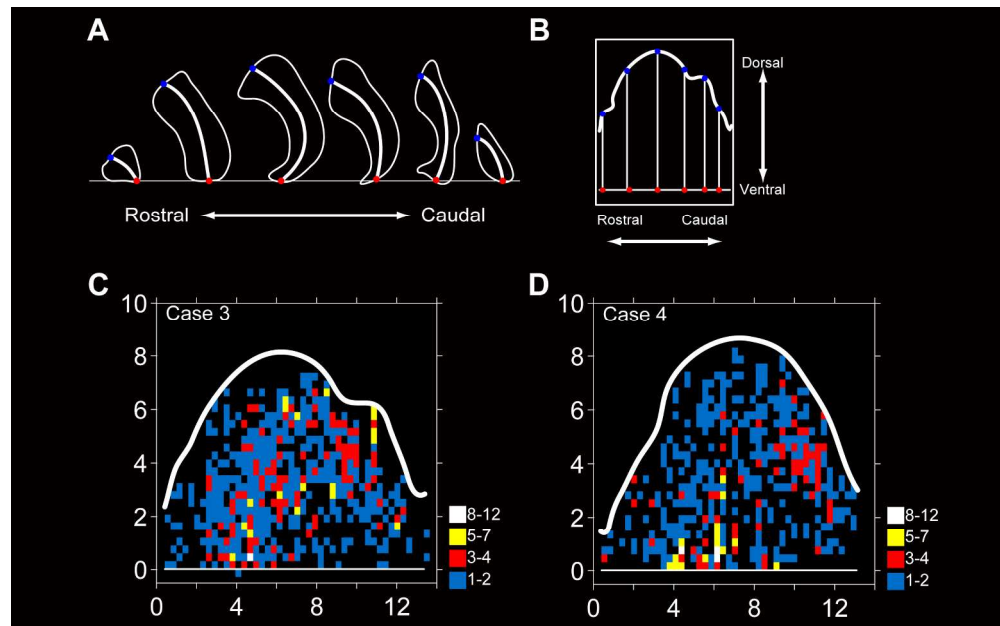


Figure 8
208x130mm (300 x 300 DPI)

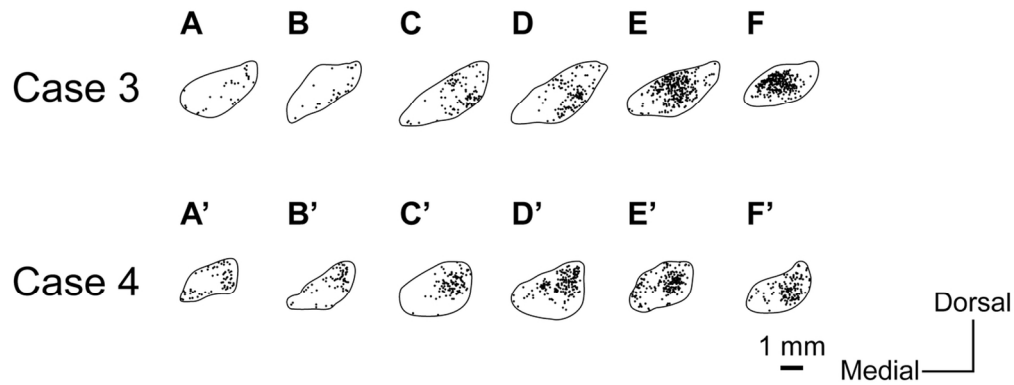


Figure 9
59x22mm (600 x 600 DPI)

Peer Review

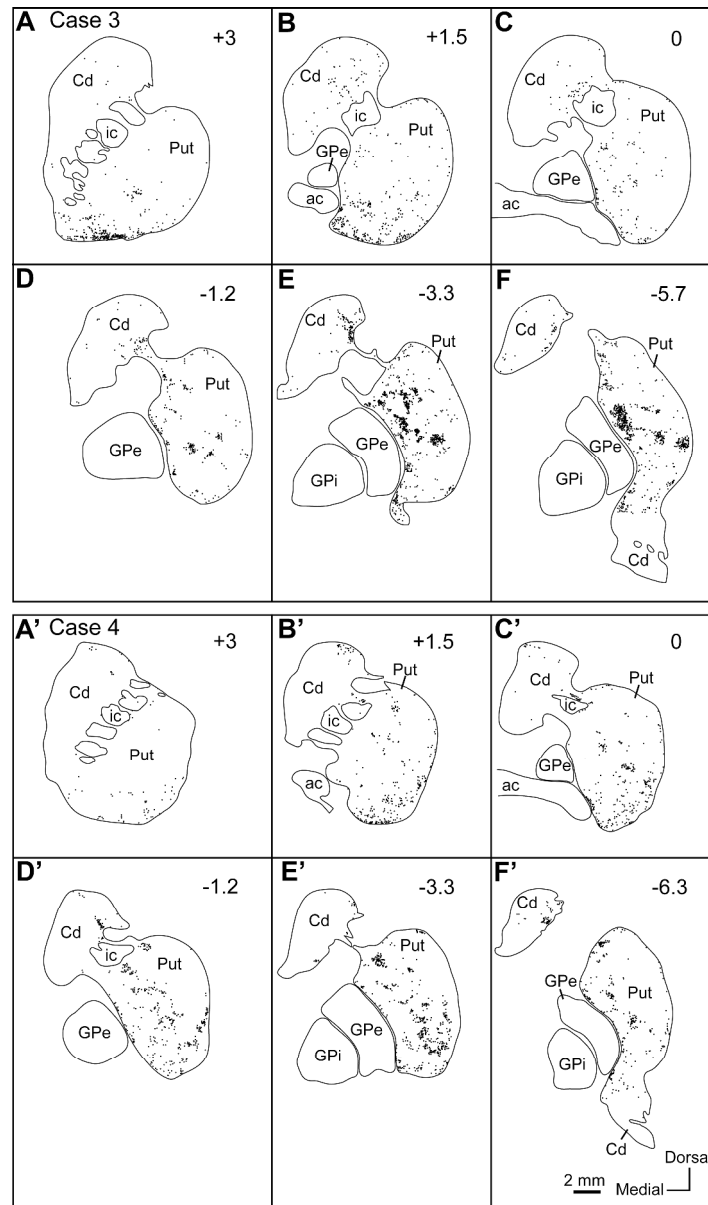
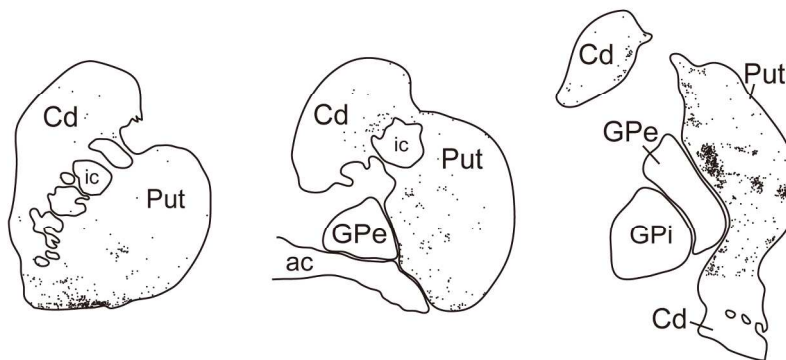
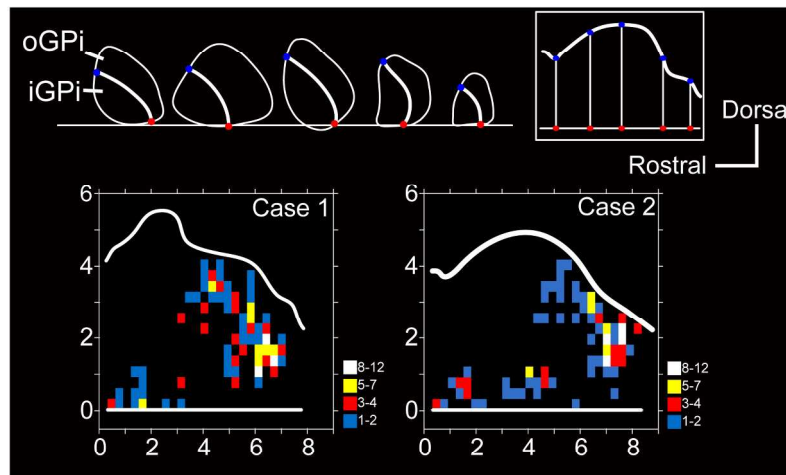
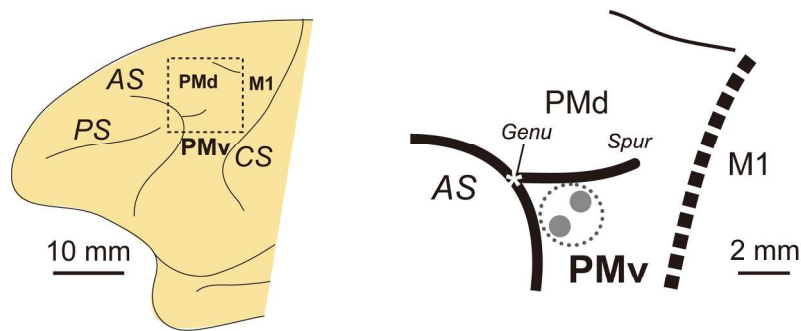


Figure 10
255x434mm (600 x 600 DPI)



159x241mm (300 x 300 DPI)

We employed retrograde transneuronal labeling with rabies virus to identify the origins of multisynaptic projections from the basal ganglia (BG) to the forelimb region of the ventral premotor cortex (PMv) in macaque monkeys. This study revealed that the PMv primarily receives major input signals from multiple territories within each structure of the BG that have comprised the two distinct motor territories (i.e., the primary and higher-order motor territories) and the limbic territory.